Rotational Perturbations in CN. Zero-Field Theory, Optical Zeeman Effect, and Microwave Transition Probabilities*

H. E. RADFORD AND H. P. BROIDA
National Bureau of Standards, Washington, D. C.
(Received May 28, 1962)

The theory of rotational perturbations in doublet states of diatomic molecules is developed and is applied to the long-standing problem of perturbations in the $B^2\Sigma^+-X^2\Sigma^+$, $v'=0$ violet bands of CN. Analysis of the available optical data yields experimental values for two rotational perturbation parameters: $(\Pi|AL_y|\Sigma)=-0.39$ cm^{-1}, $(\Pi|BL_y|\Sigma)=0.011$ cm^{-1}, which account satisfactorily for all the observed spectral line shifts. These two parameters then are used to predict the Zeeman effect of the rotational perturbations. The calculated Zeeman effects are checked against new observations of the 0, 0 band of the violet CN system at magnetic field strengths up to 28 kG, and good agreement is found between theory and experiment. Finally, the zero-field analysis is used to examine the feasibility of proposed microwave resonance investigations of the perturbed excited states of CN.

I. INTRODUCTION

THE visible band spectra of diatomic molecules sometimes exhibit rotational perturbations—irregularities in the rotational fine structure of individual bands. The perturbations are caused by an accidental near degeneracy of two rotational energy levels which belong to different electronic states of the molecule. Provided certain selection rules are fulfilled, the two close levels suffer a mutual repulsion, and each takes on partially the properties of the other; i.e., the two molecular states become mixed. The mixed properties include transition probabilities and magnetic moments. Thus, the perturbed spectral lines may exhibit peculiar intensities and Zeeman effects, as well as displacements from their expected positions in the band.

Herzberg,[1] in 1928, found some particularly fine examples of rotational perturbations in the CN $v'=0$ violet bands ($B^2\Sigma^+-X^2\Sigma^+$), using as his emission source the luminous chemical reaction produced by adding an organic vapor to active nitrogen. In subsequent spectroscopic studies of this "atomic flame" the perturbed CN levels were identified,[2] and measurements were made of their separations, their shifts, and their relative populations.[3] In recent experiments the pressure dependence of relative line intensities in the perturbed bands has been investigated in detail,[4] and precise wavelength measurements have been made on the perturbed lines.[5]

To the microwave spectroscopist seeking examples of abnormal energy level populations, one result of these experiments is especially interesting: The perturbations in the $v'=0$ bands show that several pairs of excited molecular levels, separated by microwave energies and connected by electric dipole matrix elements, can have steady-state population ratios of ten or twenty to one. Stimulated microwave transitions between these levels may well be detectable by changes in the intensity of perturbed lines in the optical spectrum. This could comprise a quite general technique of performing microwave spectroscopy on excited molecular states, applicable to any diatomic molecule whose optical spectrum exhibits rotational perturbations. The essential difference between this and conventional microwave absorption methods is in the energy of the photons which signal the microwave resonance condition. The rotational perturbation phenomenon would effectively convert the low-energy microwave photons absorbed or emitted at resonance into high-energy optical photons, which can be detected with much better sensitivity. Similar techniques have been applied successfully in studies of excited atomic states.[6]

To evaluate the feasibility of this technique, one requires information on level separations, relative populations, microwave transition probabilities, radiative lifetimes, and collisional relaxation times. Except for level separations and relative populations, this information is not available from earlier analyses of the CN rotational perturbations. As the present paper will show, the microwave transition probabilities can be derived from the measured line shifts in the optical spectrum. For this purpose a detailed quantum-mechanical analysis of rotational perturbations in spin doublet states is required, and is developed here. To provide a further test of the theory, the Zeeman effect of the perturbed lines is calculated, using molecular constants derived from the zero-field analysis. The results are checked against new experimental observations of the Zeeman effect.

In addition to splitting and shifting the perturbed lines, strong magnetic fields also are found to have a marked effect on the intensities of the perturbed CN lines. This effect, as well as the previously observed pressure dependence of relative intensities, is discussed in a forthcoming paper[7] which deals with chemical

* Supported in part by the Office of Naval Research.
[1] G. Herzberg, Z. Physik **49**, 512 (1928).
[2] H. Beutler and M. Fred, Phys. Rev. **61**, 107 (1942).
[3] A. T. Wager, Phys. Rev. **64**, 18 (1943).
[4] H. P. Broida and S. Golden, Can. J. Chem. **38**, 1666 (1960).
[5] N. H. Kiess and H. P. Broida, J. Mol. Spectroscopy **7**, 194 (1961).
[6] G. W. Series, *Reports on Progress in Physics* (The Physical Society, London, 1959), Vol. 22, p. 280.
[7] H. E. Radford and H. P. Broida, J. Chem. Phys. (to be published).

kinetic aspects of the active nitrogen atomic flame. The intensity analysis presented there yields values for the radiative and collisional lifetimes that are pertinent to the design of a microwave resonance experiment on CN.

II. THEORY OF ROTATIONAL PERTURBATIONS IN DOUBLET STATES

For most calculations of molecular energies a treatment based on the Born-Oppenheimer approximation is good enough. Electronic motion, nuclear vibration, and molecular rotation are assumed to be completely independent and the energies of the three motions, computed separately, are added to give the total energy. There are, however, certain observable features of molecular spectra which fail to be accounted for by these calculations, and it becomes necessary to consider in explicit fashion the interactions between the three types of motion. Rotational perturbations provide an example; they are caused by the interaction between electronic motion and molecular rotation. The interaction is ordinarily small, and may be computed with the quantum-mechanical perturbation theory. The theoretical discussion given below is first restricted to the zero-field case, and is then generalized to include the Zeeman effect in moderately strong magnetic fields. The zero-field analysis parallels, but carries somewhat further, the earlier work of Ittman.[8] The theoretical results are general, and can be applied to molecules other than CN; examples include the isoelectronic molecular ions N_2^+ and CO^+.

1. Zero Magnetic Field

The complete Hamiltonian of molecular rotation and fine structure in diatomic molecules contains the L-uncoupling terms

$$H_L=(A+2B)(L_xS_x+L_yS_y)-2B(J_xL_x+J_yL_y), \quad (1)$$

which are responsible for many of the finer details of molecular spectra, including Λ-type doubling, ρ-type doubling, and rotational perturbations.[8–10] The interaction between molecular rotation and internal electronic motion represented by H_L induces a component of $\mathbf{L}$ (electronic orbital angular momentum) perpendicular to the internuclear axis, in competition with the strong electrostatic forces which would otherwise require $\mathbf{L}$ to process strictly about the axis with constant projection Λ. The perpendicular component of $\mathbf{L}$ also interacts magnetically with the molecular nuclei and with external magnetic fields, contributing thereby to the molecular hyperfine structure and Zeeman effect.[11,12]

The nonvanishing matrix elements of H_L are off diagonal in Λ by one unit (i.e., $\Delta\Lambda=\pm1$) but diagonal in J and S, the quantum numbers of total angular momentum and spin. They also are diagonal with respect to the following symmetry operations: reflection at the origin (over-all + or − parity), reflection in a plane containing the internuclear axis (c or d symmetry),[13] and exchange of the nuclei, if identical (a or s symmetry).[14,15] There is no corresponding selection rule for the vibrational quantum number v, since the vibrational functions of two different electronic states are not orthogonal. Instead, a kind of Franck-Condon principle operates: The magnitude of matrix elements of H_L connecting two vibrational states, and hence the strength of the perturbation, is approximately proportional to the overlap integral $(\int\psi_v^*\psi_{v'}dr)$ of the two vibrational functions.

The essential difference between the phenomena of rotational perturbations on the one hand and Λ- and ρ-type doubling on the other lies in the size of the overlap integral. This can approach unity for vibrational states which have nearly the same vibrational quantum number, but these states are usually separated by large energies. A second-order perturbation calculation[9] shows that in this case the perturbation affects every rotational level of both vibrational states; this produces the ρ-type doubling of Σ states, the Λ-type doubling of Π or Δ states. If, on the other hand, the vibrational overlap integral is small, significant perturbations can occur only when two individual rotational levels lie very close to each other and simultaneously satisfy the selection rules concerning angular momentum and symmetry. These levels, and only these levels, will appear to have Λ- or ρ-type doublings inconsistent with those of neighboring levels: They will be "rotationally perturbed."

In a $^2\Pi-{}^2\Sigma$ perturbation any given pair of vibrational states have between them only three levels of the same J and parity, one $^2\Sigma$ level and two $^2\Pi$ levels [in Hund's case (a), these are the $^2\Pi_{1/2}$ and $^2\Pi_{3/2}$ members of a fine structure doublet]. The matrix of the perturbation Hamiltonian H_L therefore can be arranged in a checkerboard pattern of 3×3 blocks, one block for each possible combination of quantum numbers representing vibration, total angular momentum, and symmetry. An accurate diagonalization

[8] G. P. Ittman, Z. Physik **77**, 616 (1931).
[9] J. H. Van Vleck, Phys. Rev. **33**, 467 (1929).
[10] G. C. Dousmanis, T. M. Sanders, Jr., and C. H. Townes, Phys. Rev. **100**, 1735 (1955).
[11] C. H. Townes and A. L. Schawlow, *Microwave Spectroscopy* (McGraw-Hill Book Company, Inc., New York, 1955), p. 207.
[12] H. E. Radford, Phys. Rev. **122**, 114 (1961); **126**, 1035 (1962).
[13] R. S. Mulliken, Revs. Modern Phys. **3**, 94 (1931). As used in the present paper, c refers to the symmetric linear combination $\psi_c=(2)^{-\frac{1}{2}}[\psi(\Lambda\Sigma\Omega)+\psi(-\Lambda-\Sigma-\Omega)]$ and d refers to the antisymmetric linear combination $\psi_d=(2)^{-\frac{1}{2}}[\psi(\Lambda\Sigma\Omega)-\psi(-\Lambda-\Sigma-\Omega)]$.
[14] R. de L. Kronig, Z. Physik **50**, 347 (1928).
[15] G. Herzberg, *Molecular Spectra and Molecular Structure* (D. Van Nostrand Company, Inc., Princeton, New Jersey, 1950), Vol. 1, p. 280.

of the entire matrix would yield the Λ- and ρ-type doublings and rotational perturbations of all levels of the $^2\Sigma-{}^2\Pi$ system. This is, of course, impractical as well as, in general, unnecessary. For an approximation good enough to fit the CN optical data, the rotational perturbation of a given pair of levels may be calculated by diagonalizing a single 3×3 submatrix. The use of this approximation amounts to an assumption that the perturbation of a given level by all levels outside its 3×3 submatrix can be represented by the usual type of Λ- or ρ-type doubling formula.[9,10] This should be true for most molecules but, depending on the theoretical accuracy desired, it is an assumption that should be regarded critically in each application of the general results given below.

The general 3×3 submatrix is given by Van Vleck[9] in a Hund's case (a) representation. A better representation to use for a discussion of the rotational perturbations is the intermediate spin-coupling representation:

$$\psi_{c/d}{}^{(1)}=(2)^{-\frac{1}{2}}(\Sigma_{\frac{1}{2}}\pm\Sigma_{-\frac{1}{2}}),$$

$$\psi_{c/d}{}^{(2)}=\left[\frac{X+(2-\lambda)}{4X}\right]^{\frac{1}{2}}(\Pi_{\frac{3}{2}}\pm\Pi_{-\frac{3}{2}})-\left[\frac{X-(2-\lambda)}{4X}\right]^{\frac{1}{2}}(\Pi_{\frac{1}{2}}\pm\Pi_{-\frac{1}{2}}),\quad(2)$$

$$\psi_{c/d}{}^{(3)}=\left[\frac{X-(2-\lambda)}{4X}\right]^{\frac{1}{2}}(\Pi_{\frac{3}{2}}\pm\Pi_{-\frac{3}{2}})+\left[\frac{X+(2-\lambda)}{4X}\right]^{\frac{1}{2}}(\Pi_{\frac{1}{2}}\pm\Pi_{-\frac{1}{2}}),$$

where

$$\lambda=A_\Pi/B_\Pi,$$
$$X=+[4(J+1/2)^2+\lambda(\lambda-4)]^{\frac{1}{2}},$$

and A_Π and B_Π are the spin-orbit and rotational constants of the $^2\Pi$ state. The c/d notation refers to the two different types of reflection symmetry mentioned above. The upper sign choice in (2) yields a c state, the lower sign choice a d state. The parameter λ measures the extent to which molecular rotation uncouples the electron spin from the internuclear axis. In the limit $|\lambda|\rightarrow\infty$, the functions (2) reduce to their case (a) form; $\psi_{c/d}{}^{(2)}$ reduces to a $^2\Pi_{3/2}$ function and $\psi_{c/d}{}^{(3)}$ to a $^2\Pi_{1/2}$ function if λ is negative (inverted fine structure), while the connection is reversed for a positive λ (regular fine structure).

The reason for choosing the intermediate spin-coupling representation is to rid the 3×3 submatrix of off-diagonal elements which, in the case (a) matrix, are responsible for the spin uncoupling. The remaining off-diagonal elements are then solely those responsible for the rotational perturbations, and are

$$S_{c/d}{}^{12}\equiv(\psi_{c/d}{}^{(1)}|H_L|\psi_{c/d}{}^{(2)})=\left[\frac{X-(2-\lambda)}{2X}\right]^{\frac{1}{2}}\{[X-\lambda\mp(2J+1)]P-Q\},\quad(3a)$$

$$S_{c/d}{}^{13}\equiv(\psi_{c/d}{}^{(1)}|H_L|\psi_{c/d}{}^{(3)})=\left[\frac{X+(2-\lambda)}{2X}\right]^{\frac{1}{2}}\{[X+\lambda\pm(2J+1)]P+Q\},\quad(3b)$$

where

$$P\equiv(\Pi|AL_y|\Sigma),$$
$$Q\equiv(\Pi|BL_y|\Sigma),$$

and again the upper signs go with c symmetry, the lower signs with d symmetry.

In these expressions A and B represent the spin-orbit and rotational operators (*not* constants), while L_y is the component of orbital angular momentum perpendicular to the internuclear axis. Only the spin and rotational dependence of the matrix elements has been evaluated. The dependence on electronic motion and nuclear vibration, which is much more difficult to evaluate, remains in the "reduced" matrix elements P and Q which will be treated here as unknown molecular parameters. As such, they are closely related to the parameters p_Λ and q_Λ used to describe Λ-type doubling. In contrast to the Λ-type doubling parameters, however, these two rotational perturbation parameters refer to two specific molecular states. For the CN perturbations to be considered here in detail, these are the $A^2\Pi_i$, $v'=10$ and $B^2\Sigma^+$, $v'=0$ states.

The diagonal elements of the 3×3 submatrices, written in the intermediate spin-coupling representation, are the unperturbed energies of the Σ level and the two Π levels having the same total angular momentum and c/d symmetry. Evaluated from the known energy constants of CN, two of these diagonal elements, the "Σ" element and one of the "Π" elements, are found to be very nearly equal for the following angular momenta and symmetries: $(7/2;c;+)$, $(15/2;d;-)$, $(17/2;d;+)$, $(21/2;c;-)$, and $(31/2;d;-)$. These correspond with the five perturbations observable in the $v'=0$ violet spectrum.[5] The two diagonal Π matrix elements differ by a fine structure energy of $B_\Pi X$ [the same X defined in Eq. (2)] which is approximately 60 cm^{-1} for all five cases, much larger than the 1 to 5 cm^{-1} difference between the Σ element and the nearly equal Π element. The level corresponding to the "other" Π element therefore plays only a minor role in the rotational perturbation; from second-order perturbation theory it should repel the Σ level by approximately the amount $S^2/B_\Pi X$, where S is the appropriate one of the four off-diagonal matrix elements given by (3). For CN this second-order term does not exceed 0.005 cm^{-1} for any one of the five perturbations. This is smaller than the expected error

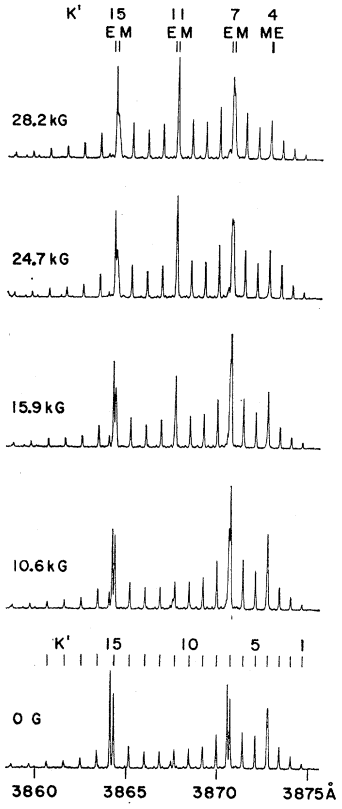

FIG. 1. The Zeeman effect of rotational perturbations in a violet band of CN. These are photoelectric recordings of the R branch of the (0, 0) band of the $B^2\Sigma^+ - X^2\Sigma^+$ electronic transition, taken in the active nitrogen flame at a total pressure of 0.6 mm Hg and at several values of magnetic field strength. Perturbed band lines from the $B^2\Sigma^+$ state are labeled "M," extra lines from the $A^2\Pi_i$ state are labeled "E."

in the line displacement measurements, and consequently we shall henceforth ignore the presence of the "other" Π level.

An exact diagonalization of the remaining 2×2 submatrix then yields the following result for the observable energy difference between the two mutually perturbing levels:

$$\Delta=[\delta^2+4S^2]^{\frac{1}{2}}, \tag{4}$$

where δ is the difference between the two nearly equal diagonal elements of the original 3×3 submatrix (i.e., δ is the separation of the "unperturbed levels") while S is again a specific one of the off-diagonal matrix elements given by (3). The correct choice of S for any particular case is a by-product of the numerical calculation of diagonal matrix elements. One finds for the CN perturbation at $J=31/2$, for instance, that the diagonal elements $(\psi_d^{(1)}|H_t|\psi_d^{(1)})$ and $(\psi_d^{(3)}|H_t|\psi_d^{(3)})$, where H_t is the complete molecular Hamiltonian, are the nearly equal ones, differing by less than 1 cm^{-1}. Thus to evaluate Δ for this case one would use S_d[13], that is, Eq. (3b) with the minus signs.

Diagonalization of the general 2×2 submatrix also yields the following normalized eigenvectors

$$\begin{aligned}\Psi^A&=(1-\rho^2)^{\frac{1}{2}}\psi_{c/d}^{(k)}-\rho^*\psi_{c/d}^{(1)},\\ \Psi^B&=\rho\psi_{c/d}^{(k)}+(1-\rho^2)^{\frac{1}{2}}\psi_{c/d}^{(1)},\end{aligned} \tag{5}$$

where

$$\rho^2=(\Delta-\delta)/2\Delta,$$

and $\psi_{c/d}^{(k)}$ stands for either $\psi_{c/d}^{(2)}$ or $\psi_{c/d}^{(3)}$ of Eq. (2). For a particular case the correct function, as well as the c/d choice, also follows from the identification of the close-lying pair of levels.

The general form of Eqs. (4) and (5) is characteristic of any interaction involving only two levels. Once this fact had been established these results could have been written down without further ado. This has been the point of view taken previously toward the CN rotational perturbations, and Eqs. (4) and (5) have been used[3,5] to derive a numerical value of S, the perturbing matrix element and of ρ^2, the wave function admixture parameter, for each perturbed line of the CN spectrum. Our reason for pursuing a more fundamental approach is to obtain general theoretical formulas for the perturbing matrix elements. These formulas, given by (3), involve only two unknown parameters, P and Q, whereas there are five observable perturbations in the CN spectrum. Thus, a systematic check of the theory is possible. The present derivation of Eqs. (4) and (5) also brings out clearly their approximate nature, and shows the sort of corrections that should be made to achieve better accuracy.

2. The Zeeman Effect

In an external magnetic field $\mathfrak{H}$ the perturbation Hamiltonian becomes H_L+Z, where

$$Z=\mu_0(\mathbf{L}+2\mathbf{S})\cdot\mathfrak{H} \tag{6}$$

except for small nuclear and virtual radiative contributions.[12] Each zero-field level splits into $2J+1$ magnetic sublevels. Some of the sublevels of the close-lying Π and Σ levels try to cross as the field is increased, but are repelled by the rotational perturbation and, at still higher fields, veer away again. The changes in the relative positions of the sublevels cause a net shift in the positions of the two levels, breaks down the selection rules for optical radiation, and produces a change in the proportions of Σ and Π character that the two states, already mixed according to Eq. (5), possess. These effects are detectable in the optical spectrum through shifts, broadenings, and intensity changes in the perturbed lines, as well as by the appearance of new spectral lines. Except for the intensity changes, discussed in reference 7, all of these phenomena are explained quantitatively by the following calculations of the Zeeman effect of perturbed lines.

Up to this point there has been no need to take account of the fact that the two levels involved in a rotational perturbation are actually doubled, the Π level being a Λ-type doublet, and the Σ level a spin (ρ-type) doublet. The reason is that the two components of a Λ-type doublet have the same total angular momentum but different parity, while the two components of a spin doublet have the same parity but differ by one unit in total angular momentum. The selection rules for rotational perturbations ($\Delta J=0$, and no change in parity) pick out just one component of

each doublet; the other two components are not perturbed, and need not be included in the perturbation matrix.

The Zeeman operator (6), (with selection rules $\Delta J=0$, ±1, and no change in parity) pulls into the perturbation matrix the other component of the spin doublet, but does not affect the other component of the Λ-type doublet. A reasonably accurate calculation of the Zeeman effect of a perturbed line therefore requires the diagonalization of a single 3×3 matrix. The necessary matrix elements of $H_P=H_L+Z$ in the intermediate spin-coupling representation are

$$
\begin{aligned}
&(\psi_c^{(1)}J|H_P|\psi_c^{(1)}J)=-m\mu_0\mathfrak{H}/(J+1),\\
&(\psi_d^{(1)}J|H_P|\psi_d^{(1)}J)=m\mu_0\mathfrak{H}/J,\\
&(\psi_c^{(1)}J|H_P|\psi_d^{(1)}J+1)=(\psi_d^{(1)}J|H_P|\psi_c^{(1)}J+1)=[(J+1)^2-m^2]^{\frac{1}{2}}\mu_0\mathfrak{H}/(J+1),\\
&(\psi_c^{(k)}J|H_P|\psi_c^{(k)}J)=(\psi_d^{(k)}J|H_P|\psi_d^{(k)}J)\\
&\qquad=\left[\frac{3}{2}\pm\frac{(2J-1)(2J+3)+3(2-\lambda)}{2X}\right]\frac{3m\mu_0\mathfrak{H}}{J(J+1)},\\
&(\psi_c^{(1)}J|H_P|\psi_d^{(k)}J-1)=(\psi_d^{(1)}J|H_P|\psi_c^{(k)}J-1)\\
&\qquad=-\left[\frac{X\pm(2-\lambda)}{2X}\frac{J-3/2}{J-1/2}(J^2-m^2)\right]^{\frac{1}{2}}(\Pi|L_y|\Sigma)\frac{\mu_0\mathfrak{H}}{2J},\\
&(\psi_c^{(1)}J|H_P|\psi_d^{(k)}J+1)=(\psi_d^{(1)}J|H_P|\psi_c^{(k)}J+1)\\
&\qquad=\left[\frac{X\pm(2-\lambda)}{2X}\frac{J+5/2}{J+1/2}((J+1)^2-m^2)\right]^{\frac{1}{2}}(\Pi|L_y|\Sigma)\frac{\mu_0\mathfrak{H}}{2(J+1)},\\
&(\psi_{c/d}^{(1)}J|H_P|\psi_{c/d}^{(2)}J)=S_{c/d}^{12}-\left[\frac{X-(2-\lambda)}{2X}\right]^{\frac{1}{2}}[X+(2-\lambda)\mp(2J+1)](\Pi|L_y|\Sigma)\frac{m\mu_0\mathfrak{H}}{J(J+1)},\\
&(\psi_{c/d}^{(1)}J|H_P|\psi_{c/d}^{(3)}J)=S_{c/d}^{13}-\left[\frac{X+(2-\lambda)}{2X}\right]^{\frac{1}{2}}[X-(2-\lambda)\pm(2J+1)](\Pi|L_y|\Sigma)\frac{m\mu_0\mathfrak{H}}{J(J+1)},
\end{aligned}
\tag{7}
$$

where m is the magnetic quantum number and $\mathfrak{H}$ is the magnetic field strength. The notation $\psi^{(k)}$ again refers to either $\psi^{(2)}$ or $\psi^{(3)}$. The upper signs are used with $k=2$ and the lower signs with $k=3$ except in the last two matrix elements, where the upper signs are used for c states and the lower signs for d states. The last two matrix elements show that the magnetic field, in addition to splitting the rotationally perturbed levels, also alters the effective strength of the rotational perturbation itself. This direct magnetic perturbation provides, in principle at least, a means of evaluating the matrix element $(\Pi|L_y|\Sigma)$ from the observed Zeeman effect. Actually, the direct magnetic perturbation is rather small compared to the rotational perturbation, and the optical Zeeman data give no information on the size of this matrix element. Its magnitude should be approximately Q/B_Σ, where B_Σ is the rotational constant of the Σ state. This estimate is used in the numerical work following.

In writing down the perturbation matrix it is convenient to choose the energy reference at the location of one of the three unperturbed levels. The unperturbed energies are then specified by two constants: the energy separation δ of Eq. (4), and the spin doubling interval δ_s, the separation of the two Σ levels. The value of δ for a particular perturbation is given by the relation $\delta=\Delta-2\epsilon$, where Δ is the actual separation of the levels and ϵ is the shift of one of the levels caused by the rotational perturbation; both of these quantities are measurable from the zero-field spectrum. The spin doubling intervals can also be estimated, although only crudely, from the optical spectrum. Fortunately the value of δ_s is small compared with δ for each of the CN levels of interest and, except at low field strengths, the Zeeman effect is relatively independent of the precise value of δ_s.

Using the matrix elements given above, and adding the values of δ and δ_s to the appropriate diagonal elements, the perturbation matrix can be written explicitly for each of the five CN perturbations. To diagonalize a given matrix requires the solution of a third-order secular equation, and so no general analytic formula can be given for the Zeeman effect. Numerical solutions can be found at various field strengths, pro-

TABLE I. Consistency check of the zero-field analysis. Comparison of measured line displacements ϵ_{exp} with calculated values ϵ_{calc} based on the parameters $Q=0.011$ cm^{-1} and $P=-0.39$ cm^{-1}. All entries in cm^{-1}.

J	Δ_{exp} [a]	S^2_{calc}	ϵ_{calc}	ϵ_{exp} [a]
7/2	0.345	0.0130	0.043	0.05
15/2	0.940	0.080	0.094	0.10
17/2	5.330	0.102	0.020	0.02
21/2	1.255	0.0021	0.018	0.02
31/2	1.285	0.290	0.291	0.28

[a] See reference 5.

vided one has numerical values of the parameters P and Q. These must first be found from an analysis of the zero-field spectrum.

III. ANALYSIS OF THE SPECTRUM

The characteristic effects of rotational perturbations on an optical band—line shifts, the presence of extra lines, anomalous intensities, and Zeeman effects—are all illustrated by Fig. 1, which shows part of the CN violet spectrum recorded at several magnetic field strengths. The "extra" lines which accompany the perturbed "main" lines are perhaps the most dramatic evidence for the sharing of observable properties by perturbed levels. The extra lines are highly forbidden (by the Franck-Condon principle) lines of the red CN band system, originating in the perturbed $A^2\Pi_i$ levels. They borrow a few percent of the transition probability of the accompanying perturbed main line, thereby increasing several hundredfold in intensity. The final state in both transitions is the same, and so the measured separations between main and extra lines gives directly the energy separations of the perturbed levels.

1. Zero Field

Measured under zero-field conditions, the separations of main and extra lines give values of Δ for use with Eq. (4). These, together with measured values of ϵ, the zero-field displacements of the main lines from their unperturbed positions, are the fundamental data that are required for a quantum mechanical analysis of the perturbations. Both Wager[3] and Kiess and Broida[5] report careful measurements of these quantities. We will use only the Kiess and Broida data in the subsequent analysis, for the following reason: As mentioned in Sec. II, the mutually perturbing levels are actually doublets, the $B^2\Sigma^+$ level a spin doublet and the $A^2\Pi_i$ level a Λ-type doublet, and only one component of each doublet engages in the perturbation. It is the separation between these two perturbing levels that is desired. The unperturbed Λ-type doublet level does not interfere with the measurement, since the corresponding transition to the ground state does not occur; that is, the extra lines are single. The main lines are unresolved doublets, however, each of whose positions correspond to the weighted mean positions of a perturbed and an unperturbed line, having relative intensities that depend on pressure. Wager's measurements, made at fairly high pressures, are somewhat unprecise for this reason. The measurements of Kiess and Broida should be more reliable because they were made at pressures low enough to make the unperturbed doublet component disappear.

The Kiess and Broida data, substituted in (3) and (4) with use of the relation $\delta=\Delta-2\epsilon$, yield the following results:

$$Q=0.011\pm0.001 \text{ cm}^{-1},$$
$$P=-0.39\pm0.04 \text{ cm}^{-1}.$$

Each is an unweighted average of three values derived from the $J=7/2$, $J=15/2$, and $J=31/2$ perturbations, which are the most sensitive to small changes in P and Q; the individual values agree to within about 10%. We use this 10% figure as a conservative estimate of uncertainty. The internal consistency of the analysis is shown by Table I, which lists the experimental values of Δ and ϵ, values of S^2 calculated with the above parameters, and values of ϵ calculated from the relation $\epsilon=[\Delta-(\Delta^2-4S^2)^{\frac{1}{2}}]/2$. The agreement between the five measured and calculated values of ϵ is quite good, and we regard this as sufficient evidence for the correctness of the analysis.

According to the pure precession hypothesis,[9] which should be reasonably valid in this case, the rotational perturbation parameter Q should be approximately equal to $B_\Sigma(\Pi|L_y|\Sigma)\simeq 2^{-\frac{1}{2}}B_\Sigma\int\psi_v^*\psi_{v'}dr$, where B_Σ is the rotational constant of the $B^2\Sigma^+$ state, equal to 2 cm^{-1}. This yields the approximate results $(\Pi|L_y|\Sigma)\simeq 0.005$, which will be used in calculating the Zeeman effect, and $\int\psi_v^*\psi_{v'}dr\simeq 0.008$, which will be used in calculating transition probabilities in Sec. IV. To a somewhat poorer approximation the parameter P can also be factored into the product $A_\Pi(\Pi|L_y|\Sigma)$ which, with the measured value $A_\Pi=-51$ cm^{-1}, gives $(\Pi|L_y|\Sigma)\simeq 0.008$, in fair agreement with the above value.

2. The Zeeman Effect

2.1 Experimental Technique

The emission source for the spectra of Fig. 1 was an atomic flame operating between the poles of an A. D. Little Bitter-type electromagnet. The reaction vessel was a 2.5 cm diam Pyrex tube, 12 cm long, fitted with two opposed gas inlet jets and a quartz window at one end and a pumping exit at the other end. One inlet jet was fed with active nitrogen produced in a 2450-Mc/sec microwave discharge; the other jet was fed with methylene chloride (CH_2Cl_2) vapor, a fuel that has been found to yield a bright, steady flame at low pressure.[16] To accommodate large flow rates, the reaction vessel was pumped by a 200-liter/sec oil ejector

[16] N. H. Kiess and H. P. Broida, *Seventh Symposium on Combustion* (Butterworth Scientific Publications, Ltd., London, 1959), p. 207.

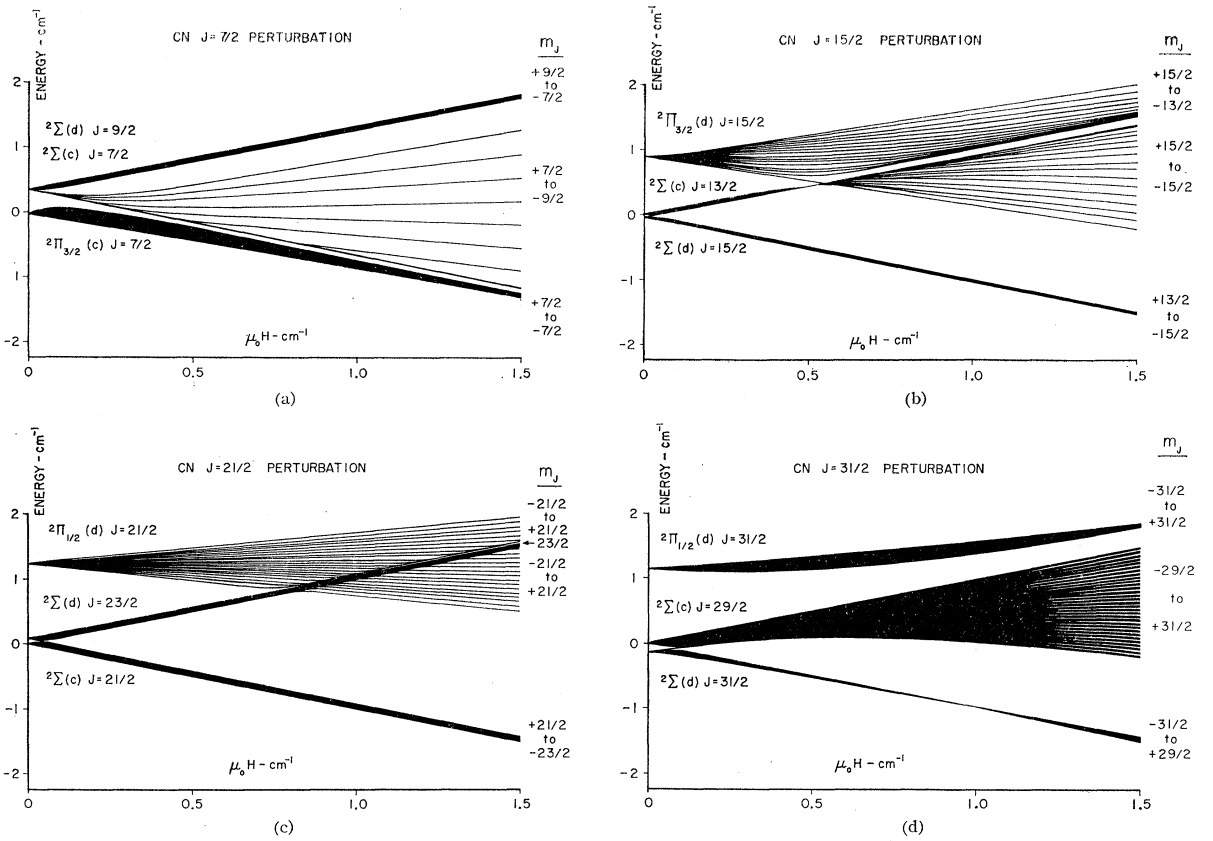

FIG. 2. (a)–(d) Calculated Zeeman splitting patterns of rotationally perturbed excited levels of CN. The vertical energy scale is referred arbitrarily to the position of one of the unperturbed levels. In each figure only one component of the $^2\Pi$ Λ-type doublet is shown. The other Λ-type doublet component does not engage in the rotational perturbation and would show only the normal linear Zeeman splitting of a $^2\Pi$ level.

pump, backed by a Kinney mechanical pump. A large liquid-nitrogen trap was included in the pumping line, to protect both pumps and personnel against the atomic flame reaction products, which include highly toxic hydrogen cyanide.

Spectra were recorded with a Leeds and Northrup grating monochrometer with photoelectric detection, the same instrument that was used in earlier work on the CN perturbations.[4,5,16] Figure 1 is a photographic reproduction of potentiometer recorder charts, recorded during relatively fast scans over the R branch of the (0, 0) violet band. Slower scans with a resolution of 0.03 Å were made over the region of the well-resolved $K'=15$ line group, to get more precise information on the Zeeman effect of the perturbed lines.

2.2 *Interpretation of the Zeeman Spectra*

Using the results of the zero-field analysis and the method of calculation outlined in Sec. II 2, the Zeeman level splitting patterns were calculated numerically for each of the five CN perturbations. The results of these numerical calculations, performed with the help of a digital computer, are plotted as a function of magnetic field strength in Figs. 2(a)–2(d). A similar plot for the $J=17/2$ case is omitted because it shows nothing but a normal Zeeman splitting at the field strengths attainable. The reason is the relatively large zero-field separation of 5.33 cm^{-1} between the perturbing Π and Σ levels for this case. A field strength in excess of 50 kG would be required to bring the magnetic sublevels of the two levels into proximity, and thereby produce repulsion effects similar to those pictured in Figs. 2(a)–2(d).

Apart from intensity variations, all the qualitative features of the Zeeman spectra can be understood from a study of Fig. 3. This is a schematic diagram of the effect of a magnetic field on both perturbed and unperturbed lines of the violet spectrum. The perturbed levels in the upper left part of the figure have been redrawn, in reduced scale, from Fig. 2(d). The two lower level patterns in Fig. 3 represent the normal Zeeman splitting of the ground state $^2\Sigma$ spin doublet levels on which the optical transitions terminate. The transitions are indicated by arrows, and are keyed to corresponding lines in the spectrum at K' values of 14 and 15. (The rotational quantum number K' is ill-defined for the perturbed lines, and is retained only as a convenient line-numbering scheme. A more precise

TABLE II. Comparison of the measured and predicted Zeeman shifts of perturbed lines in the CN $v'=0$ violet band at $K'=15$. The lines M, E, and EE are identified in Fig. 3. All entries in cm^{-1}.

H (kG)	ΔM exp	ΔE exp	ΔE calc	ΔEE exp	ΔEE calc	$\frac{1}{2}(\Delta EE+\Delta E)$ exp	$\frac{1}{2}(\Delta EE+\Delta E)$ calc	$\Delta EE-\Delta E$ exp	$\Delta EE-\Delta E$ calc
0	0	0	0	0	0	0	0	0	0
10.8	0	−0.36	−0.42	0.73	0.59	0.18	0.09	1.09	1.01
15.9	0	−0.56	−0.54	1.05	0.94	0.25	0.20	1.61	1.48
21.2	−0.07	−0.63	−0.65	1.42	1.33	0.40	0.34	2.05	1.98
24.0	−0.13	−0.69	−0.71	1.58	1.53	0.45	0.41	2.27	2.24
26.0	−0.04	−0.69	−0.74	1.75	1.70	0.53	0.48	2.44	2.44
28.2	−0.07	−0.72	−0.76	1.95	1.88	0.62	0.56	2.67	2.64

designation for the perturbed $K'=15$ lines would be $J'=31/2$.)

First consider the unperturbed case. The magnetic field splits both the upper $B^2\Sigma^+$ spin doublet level and the lower $X^2\Sigma^+$ spin doublet level equally into two groups of magnetic sublevels, corresponding to the two orientations of the spin of the unpaired electron with respect to the field direction. The selection rule $\Delta m_s=0$ for electric dipole transitions allows only the two transitions shown, and it is clear that the optical line will show essentially no Zeeman effect. Close examination of the spectrum shows that the magnetic field does have a small effect on the unperturbed lines: It closes up the spin doublet structure in lines where this structure is resolvable at zero field. Zero-field lines that are not split but only broadened by the doublet structure show a corresponding narrowing. This is a well-known phenomenon,[17] which results from the magnetic uncoupling of the electron spin from the molecular rotation.

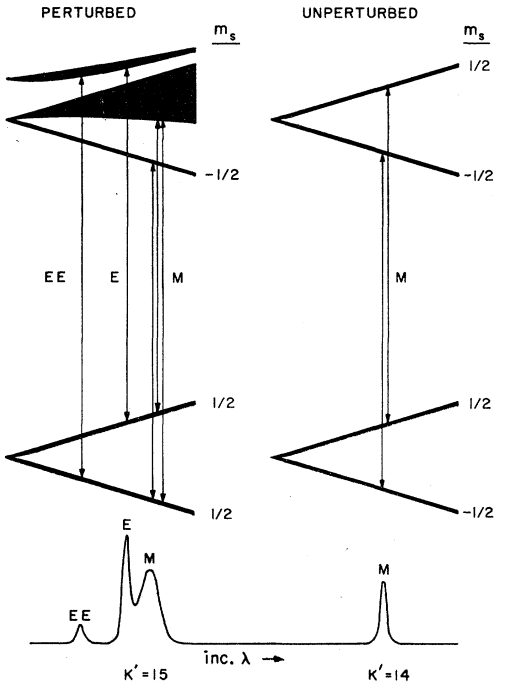

FIG. 3. Schematic explanation of the Zeeman effect of perturbed and unperturbed lines in the violet band of Fig. 1. The optical transitions are indicated by arrows, and are keyed to corresponding spectral lines in the lower part of the figure.

The Zeeman effect of perturbed lines is much more complex, as indicated by the left side of Fig. 3. The combined effect of the magnetic field and the rotational perturbation is to give the electron spin a complicated precessional motion about the direction of the field. That is, the two levels which tend to approach each other as the field is increased take on a mixed character and their wave functions must be expressed as linear combinations of the two spin states $m_s=+1/2$ and $m_s=-1/2$. Optical transitions can, in consequence, take place to either of the ground spin states. One result is that a new line (EE in Fig. 3) splits off from the extra line of each perturbation and moves away as the field is increased. A second result is that the main line broadens rapidly as the field is increased, but shows only a small net shift in position. The intensity of the EE line depends on the fractional $m_s=-1/2$ character of the upper level in Fig. 3. This intensity diminishes with increasing field strength (see Fig. 1) which indicates that the upper level becomes more and more a pure $m_s=+1/2$ level. As far as magnetic properties are concerned, then, the original Π level is converted into a Σ level by the application of a strong field. Similarly, the original Σ level takes on the magnetic properties of the Π level. This exchange of magnetic properties is also evident from the detailed energy level diagrams of Figs. 2(a)–2(d): The Π sublevels crowd together and assume the uniform slope characteristic of a Σ level while the Σ sublevels peel off into the characteristic fan of a Π level.

A quantitative check of the Zeeman effect calculations can be made against the observed shifts from their zero-field positions of the lines at $K'=15$. These shifts were measured from recorder charts taken at slow scan speeds, using the wavelength calibration provided by the neighboring unperturbed lines. The comparison between measured and calculated line shifts is given by Table II. Positive shifts mean that the line moves toward larger wave numbers (shorter wavelength) when the field is applied. The calculated line shifts are taken from Fig. 2(d), with the further assumption that the lower $^2\Sigma$ level involved in the

[17] F. H. Crawford, Revs. Modern Phys. **6**, 90 (1934).

optical transitions has essentially no spin splitting, and that, therefore, its $m_s=1/2$ and $m_s=-1/2$ sublevel groups separate linearly with magnetic field. The groups of sublevels involved in the E and EE transitions remain fairly compact at all field strengths; the corresponding lines remain sharp, and their positions can be predicted with good accuracy. This is not the case for the M line, whose apparent position represents a weighted average over individual widely separated sublevels of the upper state. Apart from the qualitative prediction, based on Fig. 3, that it will show little if any net shift, no attempt has been made to calculate the shift of the M line.

From Table II it is clear that the general behavior of the lines at $K'=15$ is consistent with the Zeeman theory, although the quantitative agreement in the measured and calculated shifts of the E and EE lines is perhaps not as good as could be expected. Errors in the measured line shifts probably do not exceed 0.05 cm^{-1}, whereas some of the discrepancies are more than twice this figure. The source of the discrepancies can be found by noting from Fig. 3 that the *separation* of the E and EE lines, $\Delta EE-\Delta E$ in Table II, gives the Zeeman splitting of the two ground levels, while the *mean shift* of the two lines $(\Delta E+\Delta EE)/2$ in Table II, gives the Zeeman shift of the upper level (except in the unlikely event that the ground levels are not split symmetrically). The tabulated values of $\Delta EE-\Delta E$ show that the splitting of the ground levels is just the expected value $2\mu_0\mathfrak{K}$, except possibly at the lower field strengths, where the neglected spin splitting may be making itself evident. The discrepancies in the measured and calculated line shifts must therefore originate in the upper level; this is borne out by the tabulated values of $(\Delta EE+\Delta E)/2$. At high field strengths the Zeeman shift of the upper level is about 0.1 cm^{-1} larger than calculated. The simplest explanation for this discrepancy is that the rotational perturbation in this case may be actually somewhat stronger than would be indicated by the measured zero-field shift $\epsilon=0.28$ cm. If this shift, which is difficult to measure at best, were actually larger by approximately 0.05 cm^{-1}, the observed Zeeman shift could be accounted for without doing violence to the consistency of the zero-field results. The accompanying changes in the derived values of P and Q would be within the 10% limit of error mentioned above.

IV. MICROWAVE TRANSITION PROBABILITIES

There are four zero-field levels in the neighborhood of each rotational perturbation: The two members of the Λ-type doublet and the two members of the spin doublet (hyperfine structure will be ignored for the time being). Optical spectra recorded at low flame pressures show that the populations of these four levels are greatly different. Stimulated microwave transitions between a given pair of these levels should tend to equalize their populations, and thereby change the intensities of corresponding lines in the optical spectrum. It is characteristic of such microwave resonance experiments on short-lived states[6] that relatively strong microwave fields are required; the reason is that the microwave transitions, in order to have an appreciable effect on the optical intensities, must be forced to occur at a rate comparable with the optical decay rate. From a calculation of the microwave transition probability one can estimate the minimum field strength required to make a given transition detectable. The success of a microwave resonance experiment then depends on whether a sufficiently powerful microwave generator is available in the appropriate frequency band, and on whether the necessary microwave power can be applied to the gaseous sample without striking an electric discharge.

The probability per unit time that a given flux of microwave energy per unit area, S_0, will induce a transition between two excited levels i and j, with reciprocal radiative lifetimes γ_i and γ_j, is approximately[6]

$$\gamma_\omega=(2\pi S_0/c\hbar^2)\times(\gamma_i+\gamma_j)|\mu_{ij}|^2/[(\omega-\omega_0)^2+\tfrac{1}{4}(\gamma_i+\gamma_j)^2], \quad (8)$$

where ω is the angular frequency of the microwave field, ω_0 is the resonant frequency $|E_i-E_j|/\hbar$, and $|\mu_{ij}|$ is the transition matrix element. This expression is derived from the time-dependent Schrödinger equation with the assumptions that the levels i and j are isolated and that γ_ω is much smaller than γ_i or γ_j. These are not serious limitations for the present purpose, which is to use Eq. (8) to estimate minimum microwave power requirements at exact resonance. The microwave line shape indicated by Eq. (8) is Lorentzian, with full width at half-maximum equal to $(\gamma_i+\gamma_j)$. This represents a minimum observable width, which would be approached in the low microwave power limit. Its numerical value determines the maximum frequency scanning rate that may be used in a microwave line search with an optical detector of given response time.

To give a detectable optical signal, the microwave transition probability at resonance, γ_{ω_0}, will have to exceed some minimum value relative to γ_i or γ_j. For the minimum power calculations we shall adopt the conservative criterion $\gamma_{\omega_0}\geq(\gamma_i+\gamma_j)/20$, a "10% transition probability" criterion. Solved for S_0, Eq. (8) then gives, at resonance,

$$S_0\geq(c\hbar^2/160\pi)[(\gamma_i+\gamma_j)^2/|\mu_{ij}|^2]. \quad (9)$$

The dipole matrix elements are

$$|\mu_{ij}|=|(\psi_i|\mathfrak{y}\cdot\mathbf{k}|\psi_j)|,$$

where $\mathfrak{y}$ is either the electric dipole moment operator

$$\mathfrak{y}_e=e\textstyle\sum_i \mathbf{r}_i$$

or the magnetic dipole moment operator

$$\mathfrak{y}=\mu_0(\mathbf{L}+2\mathbf{S}),$$

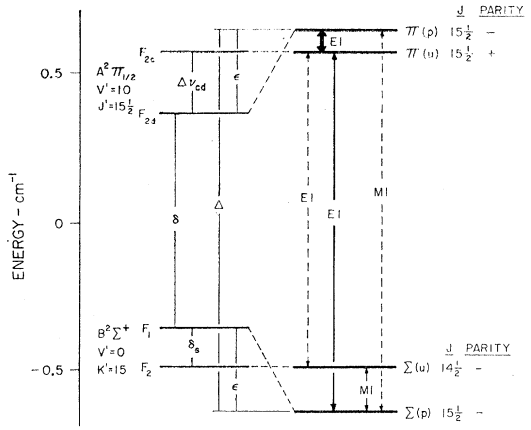

FIG. 4. Excited energy levels of CN in the neighborhood of the $J'=15\frac{1}{2}$ rotational perturbation, and predicted microwave transitions. The hypothetical unperturbed levels are shown on the left. The energy intervals δ, δ_s, Δ, and ϵ are those used in the analysis of the rotational perturbations; $\Delta\nu_{cd}$ is the unperturbed Λ-type doublet interval. Microwave transitions between actual perturbed levels on the right are indicated by arrows, drawn with differing line weights to suggest relative transition probabilities.

and $\mathbf{k}$ is the polarization vector of the applied microwave field. To correspond with the usual experimental situation we take the microwave field to be linearly polarized, and let the direction of the appropriate field vector ($\mathbf{E}$ for electric dipole transitions, $\mathfrak{IC}$ for magnetic dipole transitions) define the z axis, fixed in the laboratory. In the absence of external fields this also provides an axis of quantization, so only matrix elements of the type $\Delta m=0$ need be considered. In the summation of $|\mu_{ij}|^2$ over the degenerate m sublevels a factor of 1/3 will enter because of the choice of linear polarization. The transition probability γ_ω is, of course, independent of the direction of polarization, provided no external fields are present.

The wave functions ψ_i and ψ_j are given by Eqs. (2) and (5) for the two perturbed levels of each rotational perturbation and by Eq. (2) for the two nearby unperturbed levels. After selecting the particular wave functions appropriate to a given perturbation, the intermediate coupling dipole matrix elements may be calculated from pure case (a) matrix elements available in the literature.[10,18,19] The computations are straightforward but somewhat tedious, and detailed formulas will not be given here. Some general aspects of the results are discussed below, and numerical values of the matrix elements are presented in Table III. The level structure and the allowed transitions for the case $J=31/2$ are shown in Fig. 4.

Electric dipole matrix elements. These vanish unless the two states have opposite parity. Among the four levels corresponding to a given perturbation the only allowed electric dipole transitions are therefore those connecting the unperturbed Π level with the perturbed Π level, with the perturbed Σ level, and with the unperturbed Σ level. There are two general types of matrix elements involved: $(\psi_c^{(k)}|\mu_{ez}|\psi_d^{(k)})$ which is proportional to the *permanent* electric dipole moment of the $A^2\Pi_i$ state, and $(\psi_{c/d}^{(k)}|\mu_{ez}|\psi_{c/d}^{(1)})$ which is proportional to the electric dipole *transition* moment for the electronic transition $A^2\Pi_i \rightarrow B^2\Sigma^+$, multiplied by the overlap integral of the $v'=10$ and $v'=0$ vibrational functions. The size of the transition moment relative to the permanent moment is not known, but the overlap integral, according to the analysis of Sec. III, has the small value 0.008. Provided the transition moment does not greatly exceed the permanent moment in size, the case (a) matrix elements of the Π-Σ type therefore can be neglected in comparison with those of the Π-Π type. This eliminates cross terms in $|\mu_{ij}|^2$, leaving $|\mu_{ij}|^2\simeq(1-\rho^2)|\psi_c^{(k)}|\mu_{ez}|\psi_d^{(k)}|^2$ for transitions between the unperturbed Π level and the perturbed Π level, and $|\mu_{ij}|^2\simeq\rho^2|(\psi_c^{(k)}|\mu_{ez}|\psi_d^{(k)})|^2$ for transitions between the unperturbed Π level and the perturbed Σ level. The first factor in these expressions is the fractional Π character of the perturbed levels; the second factor is the squared matrix element for Λ-type doubling transitions, given by Eq. (39) of reference 10.

The results for electric dipole transitions may be summarized as follows: Transitions between the two perturbed levels of a given rotational perturbation are forbidden rigorously by parity selection rules. Transitions between the two *un*perturbed levels are highly unlikely because of the small vibrational overlap, and for most practical purposes can be considered forbidden also. The observable electric dipole spectra will be Λ-type doubling transitions between the two Π levels and between the unperturbed Π level and the perturbed Σ level. The latter transitions are possible only because of the rotational perturbation, which admixes some Π character into the perturbed Σ level.

TABLE III. Calculated dipole matrix elements of transitions in the microwave spectrum of the CN rotational perturbations.

Transition[a]	J	$\lvert\mu_{ij}\rvert^2$ (electric dipole)	$\lvert\mu_{ij}\rvert^2$ (magnetic dipole)
$\Pi(u)-\Pi(p)$	7/2	$2.3\times10^{-1}\,\mu^2/3$	
	15/2	1.6×10^{-2}	
	21/2	1.0×10^{-3}	
	31/2	4.7×10^{-4}	
$\Pi(u)-\Sigma(p)$	7/2	$2.5\times10^{-2}\,\mu^2/3$	
	15/2	2.3×10^{-3}	
	21/2	5.1×10^{-5}	
	31/2	1.9×10^{-4}	
$\Sigma(u)-\Sigma(p)$	all J		$\sim\mu_0^2/3$
$\Pi(p)-\Sigma(p)$	7/2		$0.05\,\mu_0^2/3$
	15/2		0.01
	21/2		~0
	31/2		~0

[a] The notation (u) and (p) means "unperturbed" and "perturbed," respectively.

[18] R. A. Frosch and H. M. Foley, Phys. Rev. **88**, 1337 (1952).
[19] C. C. Lin and M. Mizushima, Phys. Rev. **100**, 1726 (1955).

Magnetic dipole matrix elements. These vanish unless the two states have the *same* parity. At each perturbation, then, transitions which involve the unperturbed Π level are rigorously forbidden. The case (a) matrix elements which correspond to Π-Σ electronic transitions are again small compared with diagonal elements, because of the small vibrational overlap, and may be neglected in a first approximation. The fully allowed transitions in this case are spin-reorientation transitions, which take place between the two Σ levels. Because of the rotational perturbation, spin-reorientation transitions are also allowed to a small extent (proportional to ρ^2) between the two perturbed levels.

Table III gives the calculated squared dipole matrix elements which are large enough to be of practical interest, and which also correspond to transitions between levels which have large population differences in the CN atomic flame. The squared matrix elements are given in units of $\mu^2/3$ for electric dipole transitions, where μ is the permanent dipole moment of the $A^2\Pi_i$ state, and in units of $\mu_0^2/3$ for magnetic dipole transitions, where μ_0 is the Bohr magneton, $e\hbar/2mc$. The factors of 1/3 account for the assumed linear polarization of the microwave field. In an isotropic microwave field these factors would become unity. The size of the electric dipole moment μ is not known, but for the purpose of calculating minimum power requirements a rough estimate will serve. On the basis of electronegativity arguments,[20] one would expect the dipole moment of CN to be nearly equal to that of NO, which, in its ground $^2\Pi$ state, has the dipole moment $\mu(\mathrm{NO};{}^2\Pi)=0.16\times10^{-18}$(cgs).[21] We shall take $\mu(\mathrm{CN};{}^2\Pi)=0.2\times10^{-18}$(cgs) in the following power calculations.

The remaining information required by Eq. (9) are the values of the reciprocal radiative lifetimes γ_i and γ_j. The radiative lifetime of the $B^2\Sigma^+$ state as a whole has been measured by a pulse excitation method[22] to be $\gamma_\Sigma^{-1}=(8.5\pm0.6)\times10^{-8}$ sec; to a sufficient approximation this may also be taken as the lifetime of a single unperturbed rotational level of the $B^2\Sigma^+$ state. From an analysis of line intensities given in reference 7 the lifetime of an unperturbed $B^2\Sigma^+$ level relative to that of an unperturbed $A^2\Pi_i$ level is found to be 0.15. For the unperturbed levels, then, $\gamma_\Sigma=1.2\times10^7$ sec^{-1} and $\gamma_\Pi=1.8\times10^6$ sec^{-1}. The perturbed levels have reciprocal radiative lifetimes intermediate between these values, given by $\gamma_\Pi+\rho^2(\gamma_\Sigma-\gamma_\Pi)$ for perturbed Π states and $\gamma_\Sigma-\rho^2(\gamma_\Sigma-\gamma_\Pi)$ for perturbed Σ states.

Minimum values of S_0 calculated from Eq. (9) are given in Table IV, together with the predicted widths and resonance frequencies of the corresponding microwave lines. The resonance frequencies are rather crude estimates based on optical data, and may be in error by as much as ±500 Mc/sec. This uncertainty is due mostly to poor knowledge of the locations of the unperturbed levels relative to the perturbed levels. The separations of the perturbed levels themselves, the values of Δ in Table I, are known rather accurately, but, unfortunately, there are no observable microwave transitions which connect these levels. Electric dipole transitions are rigorously forbidden, and the weak spin-reorientation transitions would require excessively large amounts of microwave power.

TABLE IV. Predicted microwave resonance properties of the CN rotational perturbations. Values of the minimum required microwave energy flux, $(S_0)_{\min}$, are calculated from Eq. (9) of the text, neglecting hyperfine structure.

Transition[a]	J	$(S_0)_{\min}$ (W/cm^2)	$\Delta\nu_{\min}$[b] (Mc/sec)	ν_0[c] (kMc/sec)
$\Pi(u)-\Pi(p)$	7/2	0.06	0.8	0.6
	15/2	0.8	0.7	2.1
	21/2	9	0.6	2.6
	31/2	40	0.9	2.1
$\Pi(u)-\Sigma(p)$	7/2	3	1.9	9.6
	15/2	37	2.1	26.1
	21/2	>1500	2.3	35.0
	31/2	300	1.8	36.5
$\Sigma(u)-\Sigma(p)$	7/2	110	3.8	0.6
	15/2	110	3.8	1.0
	21/2	110	3.8	2.3
	31/2	110	3.8	4.5

[a] The notation (u) and (p) means "unperturbed" and "perturbed," respectively.
[b] Full microwave linewidth at half-maximum intensity, calculated from measured optical decay lifetimes.
[c] Estimated from optical data given in references 3 and 4. These resonance frequencies may be in error by as much as 0.5 kMc/sec.

The maximum flux of microwave energy that can be applied to the CN atomic flame without striking a gas discharge will depend on experimental conditions, but at best it seems doubtful that the gas could withstand much over 100 W/cm^2. The prospects of detecting the magnetic dipole transitions listed in Table IV are therefore uncertain, although certainly not hopeless. Equation (9) and all the entries in Table IV are based on a 10% microwave transition probability, an estimate that may be too large by one or two orders of magnitude. The magnetic dipole transitions are especially worth searching for because, as shown by the optical spectrum, a large number of the spin doublet levels have unequal populations, not just those at the rotational perturbations. Essentially the same microwave power level would be required for all the spin doublet transitions, perturbed and unperturbed. Thus it may be possible to measure, by the microwave resonance method, the spin doublet separations and hyperfine structure of most of the rotational lines in the $v'=0$ violet band.

Unquestionably the best transitions to investigate first are the three electric dipole transitions at 0.6, 2.1, and 9.6 kMc/sec. The power requirements of the two lower frequency transitions are well within the range of broad-band uhf power sources. The power require-

[20] L. Pauling, *The Nature of the Chemical Bond* (Cornell University Press, Ithaca, 1960), p. 97.
[21] L. G. Wesson, *Tables of Electric Dipole Moments* (Technology Press, Cambridge, Massachusetts, 1948).
[22] R. G. Bennet and F. W. Dalby, J. Chem. Phys. **36**, 399 (1962).

ment of the high-frequency transition can be met by a moderate-power magnetron feeding a horn radiator or a klystron feeding a resonant cavity (within which the atomic flame could be operated). The necessary klystron power depends on the quality factor (Q) and volume (V) of the resonant cavity, according to the approximate relation

$$P=2\pi S_0 V\nu_0/cQ. \quad (10)$$

For the typical values $V=10^2$ cm^3 and $Q=5\times10^3$, the klystron power required for a 10% transition probability at 9.6 kMc/sec is 125 mW. This is easily obtained from standard X-band klystrons.

Finally, a word about hyperfine structure. The CN microwave transitions should show a well-resolved splitting into three major hyperfine components, especially at the lower J values, because of magnetic interactions between the uncompensated electronic angular momenta and the magnetic moment of the nitrogen nucleus. (N^{14} also possesses an electric quadrupole moment, and the resulting quadrupole interaction may also be detectable through small line shifts.) The intensities of the three hyperfine components should be more or less equal, so, to be on the safe side, one should multiply the results of the minimum power calculations by three. Thus, a 375-mW klystron might be necessary for an investigation of the 9.6-kMc/sec spectrum.

PHYSICAL REVIEW VOLUME 128, NUMBER 1 OCTOBER 1, 1962

Recoil Studies of Reactions of Indium with Medium Energy Protons and Alpha Particles*

N. T. PORILE, A. M. POSKANZER, AND M. RHO†
Chemistry Department, Brookhaven National Laboratory, Upton, New York
(Received May 7, 1962)

Recoil ranges projected along the beam direction have been measured for the $(\alpha,\alpha\gamma)$, $(\alpha,\alpha n)$, (α,pn), and $(p,p\gamma)$ reactions on In^{115} and for the $In^{113}(p,n)$ reaction, with 5 to 10 MeV protons and 20 to 40 MeV alpha particles. The results have been compared with values expected for compound-nucleus formation and reasonable agreement is obtained for the (α,pn), $(p,p\gamma)$, and (p,n) reactions. The measured range for the $(\alpha,\alpha n)$ reaction agrees with calculation at the lowest energy studied but is somewhat low at the highest bombarding energy. In the case of the $(\alpha,\alpha\gamma)$ reaction the measured ranges are a factor of 3 to 6 smaller than the calculated values, indicating a direct interaction process. The recoil ranges expected for Coulomb excitation have been computed for the $(\alpha,\alpha\gamma)$ and $(p,p\gamma)$ reactions and are substantially smaller than the experimental values. Excitation function measurements for the (α,pn) reaction are also presented.

I. INTRODUCTION

EXCITATION-FUNCTION measurements for reactions of In^{115} with medium-energy alpha particles, deuterons, and protons have been reported recently.[1] In particular, cross sections for the formation of In^{115m} were obtained for all the above bombarding particles. The cross sections for the $(\alpha,\alpha\gamma)$ reaction were compared in detail with the statistical theory and a definite disagreement was found for bombarding energies above 25 MeV. The contribution of the Coulomb excitation process was estimated and found to be substantial, particularly below 25 MeV. It was impossible to draw definite conclusions about the mechanism responsible for the other reactions leading to the formation of In^{115m}. This same uncertainty also applied to the $In^{115}(\alpha,\alpha n)$ In^{114m} reaction whose excitation function was also obtained in that study.

In order to obtain additional information about some of the above reactions, an investigation of the recoil properties of the reaction products has been carried out.[2] The fraction of activity recoiling in the forward direction out of a target thick compared with the recoil range has been measured for the following reactions: $In^{115}(\alpha,\alpha\gamma)In^{115m}$, $In^{115}(\alpha,\alpha n)In^{114m}$, $In^{115}(\alpha,pn)Sn^{117m}$, $In^{115}(p,p\gamma)In^{115m}$, and $In^{113}(p,n)Sn^{113}$. In addition, the excitation function for the (α,pn) reaction has also been obtained. Previous measurements of this type have been carried out in this energy range for reactions of alpha particles with aluminum,[3] potassium,[4] bismuth,[5] as well as for a number of heavy ion induced reactions.[6]

II. EXPERIMENTAL PROCEDURE AND RESULTS

The target foils consisted of natural indium evaporated to a thickness of 1 to 2 mg/cm^2 onto high-purity

* Research performed under the auspices of the U. S. Atomic Energy Commission.
† Present address: Lawrence Radiation Laboratory, University of California, Berkeley, California.
[1] N. T. Porile, Phys. Rev. **121**, 184 (1961).
[2] A preliminary account of this investigation has appeared in Bull. Am. Phys. Soc. **7**, 83 (1962).
[3] N. T. Porile, Phys. Rev. **127**, 224 (1962).
[4] T. Matsuo and T. T. Sugihara, Can. J. Chem. **39**, 697 (1961).
[5] B. G. Harvey, W. H. Wade, and P. F. Donovan, Phys. Rev. **119**, 225 (1960).
[6] L. Winsberg and J. M. Alexander, Phys. Rev. **121**, 518 (1961); J. M. Alexander and L. Winsberg, Phys. Rev. **121**, 529 (1961).